

Energy transfer in colloidal CdTe quantum dot nanoclusters

Clare Higgins,¹ Manuela Lunz,¹ A. Louise Bradley,^{1,*} Valerie A. Gerard,²
Stephen Byrne,² Yurii K. Gun'ko,² Vladimir Lesnyak,³ and Nikolai Gaponik³

¹Semiconductor Photonics group, School of Physics, Trinity College Dublin, Dublin 2, Ireland

²School of Chemistry, Trinity College Dublin, Dublin 2, Ireland

³Physical Chemistry, TU Dresden, Bergstr. 66b, 01062 Dresden, Germany

*bradlei@tcd.ie

Abstract: Quantum dot (QD) nanoclusters were formed using oppositely charged colloidal CdTe QDs, of two different sizes, mixed in aqueous solutions. The photoluminescence (PL) spectra and time-resolved PL decays show signatures of Förster resonant energy transfer (FRET) from the donor QDs to the acceptor QD in the nanoclusters. A concentration dependence of the donor QD lifetime is observed in mixed solutions with a donor: acceptor ratio greater than 1:1. The concentration dependent time-resolved PL data indicate different regimes of cluster formation, with evidence for donor-to-donor FRET in the larger donor-acceptor nanoclusters and evidence for the formation of all-donor clusters in mixed solutions with high donor concentrations.

©2010 Optical Society of America

OCIS codes: (160.4236) Nanomaterials; (250.5230) Photoluminescence; (160.4760) Optical properties; (260.2160) Energy transfer; Nanocrystals; Nanoassemblies; Quantum dots.

References and links

1. I. L. Medintz, A. R. Clapp, H. Mattoussi, E. R. Goldman, B. Fisher, and J. M. Mauro, "Self-assembled nanoscale biosensors based on quantum dot FRET donors," *Nat. Mater.* **2**(9), 630–638 (2003).
2. T. Franzl, T. A. Klar, S. Schietinger, A. L. Rogach, and J. Feldmann, "Exciton recycling in graded gap nanocrystal structures," *Nano Lett.* **4**(9), 1599–1603 (2004).
3. T. Förster, "Zwischenmolekulare Energiewanderung und Fluoreszenz," *Annalen der Physik* **437**(2), 55–75 (1948).
4. A. R. Clapp, I. L. Medintz, and H. Mattoussi, "Förster resonance energy transfer investigations using quantum-dot fluorophores," *ChemPhysChem* **7**(1), 47–57 (2006).
5. E. Alghandery, L. M. Walsh, Y. Rakovich, A. L. Bradley, J. F. Donegan, and N. Gaponik, "Highly efficient Förster resonance energy transfer between CdTe nanocrystals and Rhodamine B in mixed solid films," *Chem. Phys. Lett.* **388**(1-3), 100–104 (2004).
6. M. Lunz, A. L. Bradley, W.-Y. Chen, and Y. K. Gun'ko, "Two-Dimensional Förster Resonant Energy Transfer in a Mixed Quantum Dot Monolayer: Experiment and Theory," *J. Phys. Chem. C* **113**(8), 3084–3088 (2009).
7. D. M. Willard, T. Mutschler, M. Yu, J. Jung, and A. Van Orden, "Directing energy flow through quantum dots: towards nanoscale sensing," *Anal. Bioanal. Chem.* **384**(3), 564–571 (2006).
8. I. L. Medintz, A. R. Clapp, J. S. Melinger, J. R. Deschamps, and H. Mattoussi, "A reagentless biosensing assembly based on quantum dot-donor Förster resonance energy transfer," *Adv. Mater. (Deerfield Beach Fla.)* **17**(20), 2450–2455 (2005).
9. P. T. Snee, R. C. Somers, G. Nair, J. P. Zimmer, M. G. Bawendi, and D. G. Nocera, "A ratiometric CdSe/ZnS nanocrystal pH sensor," *J. Am. Chem. Soc.* **128**(41), 13320–13321 (2006).
10. T. Pons, I. L. Medintz, M. Sykora, and H. Mattoussi, "Spectrally resolved energy transfer using quantum dot donors: Ensemble and single-molecule photoluminescence studies," *Phys. Rev. B* **73**(24), 245302 (2006).
11. E. Mutlugun, O. Samarskaya, T. Ozel, N. Cicek, N. Gaponik, A. Eychmüller, and H. V. Demir, "Highly efficient nonradiative energy transfer mediated light harvesting in water using aqueous CdTe quantum dot antennas," *Opt. Express* **18**(10), 10720–10730 (2010).
12. R. Wargnier, A. V. Baranov, V. G. Maslov, V. Stsiapura, M. Artemyev, M. Pluot, A. Sukhanova, and I. Nabiev, "Energy transfer in aqueous solutions of oppositely charged CdSe/ZnS core/shell quantum dots and in quantum dot-nanogold assemblies," *Nano Lett.* **4**(3), 451–457 (2004).
13. R. Osovsky, A. Shavel, N. Gaponik, L. Amirav, A. Eychmüller, H. Weller, and E. Lifshitz, "Electrostatic and covalent interactions in CdTe nanocrystalline assemblies," *J. Phys. Chem. B* **109**(43), 20244–20250 (2005).

14. S. Mayilo, J. Hilhorst, A. S. Susa, C. Höhl, T. Franzl, T. A. Klar, A. L. Rogach, and J. Feldmann, "Energy transfer in solution-based clusters of CdTe nanocrystals electrostatically bound by calcium ions," *J. Phys. Chem. C* **112**(37), 14589–14594 (2008).
15. Z. Tang, B. Ozturk, Y. Wang, and N. A. Kotov, "Simple Preparation Strategy and One-Dimensional Energy Transfer in CdTe Nanoparticle Chains," *J. Phys. Chem. B* **108**(22), 6927–6931 (2004).
16. M. Lunz, A. L. Bradley, W. Chen, V. A. Gerard, S. J. Byrne, and Y. K. Gun'ko, "Influence of quantum dot concentration on Förster resonant energy transfer in monodispersed nanocrystal quantum dot monolayers," *Phys. Rev. B* **81**(20), 205316 (2010).

1. Introduction

Recent growth in the areas of bio-sensing and solar cells has led to increased interest in composite nano-assemblies with light harvesting capabilities [1,2]. These structures employ Förster resonant energy transfer (FRET) to generate energy flow from an energy donor to an energy acceptor. FRET is an energy transport mechanism that occurs on the nanoscale via dipole-dipole interactions. Factors influencing the energy transfer include spectral overlap of the emission spectrum of the donor with the absorption spectrum of the acceptor and the distance between the donor and acceptor. The distance at which the FRET efficiency is 50% is called the Förster radius (R_0), typically in the range of 1 – 10 nm [3]. FRET occurs naturally in biological systems but can also be artificially engineered. Traditional fluorophores have been utilised as donors and acceptors in FRET systems, however narrow excitation windows and broad emission bands can lead to cross-talk between donor and acceptor signals, complicating the analysis. Additionally, these fluorophores are prone to issues with photobleaching and photostability [4]. Due to their unique optical properties, such as a narrow, tuneable emission features, broad absorption bands and high quantum yields, colloidal semiconductor Quantum Dots (QDs) are of significant interest as energy donors and acceptors for FRET nano-assemblies [5]. FRET between donor and acceptor QDs has previously been investigated in a variety of structures and geometries. It has been shown that the FRET efficiency and the acceptor enhancement can be tuned by varying the donor: acceptor concentration ratio in randomly mixed donor – acceptor QD monolayers [6].

Solution based assemblies of donor and acceptor species interacting via FRET can be used as the basis for nano-sensors, monitoring the changes in the FRET signatures, such as donor emission quenching or acceptor enhancement, upon creation or disruption of energy flow due to binding or ligand exchange [3,7] or conformational changes [8,9]. Due to their unique optical properties, QDs have been proposed as building blocks, often the scaffold for such nanosensors [1,7]. In order to optimize the performance of these sensors, detailed investigation of FRET between donors and acceptors in QD nano-assemblies are necessary to determine the factors that influence the sensitivity of the sensors. It is furthermore important to find easy ways of monitoring the assembly of these structures.

Nanoscale clusters provide the opportunity to investigate FRET on the single donor or acceptor scale. Reports for donor QD – acceptor dye structures with multiple acceptors per donor QD, have shown that strong FRET signatures are observed for optimized spectral overlap of the donor emission and acceptor absorption [10,11]. For ensembles of these single donor QD structures a strong wavelength dependence of the FRET rate was observed, due to varying spectral overlap over the QD ensemble [10]. Therefore it is important to investigate the impact of the inhomogeneous broadening of the donor QDs in a multiple donor QD – single acceptor structure. Apart from numerous investigations of QD – dye systems, FRET has also been observed in nanoclusters of electrostatically bonded oppositely charged CdSe/ZnS QDs [12]. Nanoclusters of CdTe nanocrystals formed by covalent and electrostatic interactions have also been investigated [13,14]. The close proximity of the QDs in nanoclusters and one-dimensional chains of nanocrystals gives rise to strong FRET signatures in the PL and time-resolved photoluminescence (TRPL) data [15]. Here we present the TRPL data for mixed solutions of oppositely charged colloidal CdTe QDs for a range of donor: acceptor concentration ratios varying from 0.28 to 12.1 donor QDs per acceptor QD. The

concentration dependence of the TRPL data shows clear evidence for donor-donor energy transfer in the solutions containing oppositely charged donor and acceptor QDs. From the donor TRPL data different regimes of cluster formation, dominated by single donor-acceptor clusters, multiple donor-acceptor clusters as well as the additional formation of donor-only clusters, are identified and discussed. Donor TRPL measurements are proposed as a quick and simple means for monitoring the formation of the nanoclusters. It can be difficult to directly access information on the clusters formed using imaging techniques such as TEM. Complicating factors include the fact that both the donor and acceptor QDs are of the same material and have with a range of possible sizes within their inhomogeneously broadened distributions. Therefore, it can be difficult to distinguish between a cluster formed from only donor QDs and one formed from an acceptor with multiple donor quantum dots attached. Additionally, it has been observed that the QDs tend to aggregate on the TEM grid and therefore the observations may not correspond to the distribution of clusters in solution. TRPL measurements, which can be performed directly on the nanoclusters in solution provide a more convenient and direct method for analysing cluster formation.

2. Experimental

QD nanoclusters were formed using oppositely charged QDs, of two different sizes, mixed in aqueous solutions. The negatively charged thioglycolic acid stabilized CdTe QDs (TGA-QDs), with a diameter of 2.4 nm and emission peak at 540 nm, act as the energy donor. The positively charged cysteamine stabilized CdTe QDs (cys-QDs), with a diameter of 3.8 nm and emission peak at 647 nm, act as the energy acceptor. The quantum yields of the TGA-QDs and the cys-QDs are 7.0% and 3.0% respectively. Positively charged cysteamine stabilised QDs generally have lower stability and lower quantum yield as the Cd-cysteamine complex is not as strong as Cd-TGA for example. Cysteamine stabilized CdTe QDs are most stable for sizes corresponding to an emission wavelength of approximately 600 nm. Therefore, fairly small TGA stabilized QDs, with a diameter 2.4 nm, were selected to act as donor QDs in order to obtain good spectral overlap with the acceptor absorption while also maintaining a good spectral separation of the TGA donor and cysteamine acceptor emission peaks allowing the FRET signatures to be clearly observed. The smaller green emitting TGA stabilised QDs exhibit relatively low quantum yields due to the trade-off between CdTe crystal size and luminescence. The zeta potentials of the positively charged acceptor cys-QDs and negatively charged donor TGA-QDs were measured to be + 60 mV and -16 mV, respectively. Dilute QD solutions were prepared and subsequently mixed to achieve donor: acceptor QD ratios from 1.3:1 to 12.1:1. The TGA-QD concentrations were varied from 9.4×10^{-7} M to 91.0×10^{-7} M, with a constant acceptor concentration of 7.5×10^{-7} M. To study the lower donor: acceptor ratios from 0.28:1 to 1.5:1 the mixed solutions were prepared using a higher acceptor QD concentration of 27.5×10^{-7} M. The corresponding donor concentrations for these solutions range from 7.7×10^{-7} M to 41.3×10^{-7} M. Solutions of pure TGA-QDs with added volumes of aqueous solutions of cys-HCl (Cysteamine hydrochloride > 97% MW 113.61, Sigma-Aldrich) were also studied. TGA-QD monolayers with a range of QD concentrations were prepared using the layer-by-layer technique [6,16]. Characterization of the monolayers sheds further light on the influence of intra-ensemble energy transfer, which will be discussed later.

A Cary 50 UV-Vis spectrometer was used to record the absorption spectra. Room temperature PL spectra were recorded using a Perkin-Elmer LS55 fluorescence spectrometer at an excitation wavelength of 400 nm. TRPL decays were measured using a PicoQuant Microtime200 time-resolved confocal microscope system with 150 ps resolution. A LDH-480 laser head controlled by a PDL-800B driver (PicoQuant) provided picosecond pulses at 470 nm for excitation. The decays were recorded with a 5 MHz repetition rate and measured over an area of $80 \times 80 \mu\text{m}$ (150×150 pixels) with an integration time of 4 ms per pixel. A

broadband filter, centred at 500 nm with a full-width half maximum of 70 nm, was used for all measurements of the donor TGA-QD TRPL in both pure and mixed solutions. A broadband filter, centred at 700 nm with a full-width half maximum of 50 nm, was used to isolate the acceptor cys-QD TRPL. The time-dependent intensity decays $I(t)$ were fitted with a two-exponential decay function given by Eq. (1)

$$I(t) = I_1 \exp(-t/\tau_1) + I_2 \exp(-t/\tau_2) \quad (1)$$

where two decay times τ_1 and τ_2 with the respective intensity weights I_1 and I_2 were taken into account. The average decay lifetime, τ_{av} , is calculated as intensity weighted means given below in Eq. (2)

$$\tau_{av} = \frac{I_1 \tau_1^2 + I_2 \tau_2^2}{I_1 \tau_1 + I_2 \tau_2}. \quad (2)$$

The error of the extracted lifetimes is less than 0.5 ns.

3. Results & Discussion

The properties of the pure QD solutions are presented first, followed the study of FRET in the nanoclusters formed in the mixed solutions. The average lifetime of the donor QDs in the mixed solutions is discussed as a function of donor:acceptor ratio, achieved by varying the donor QD concentration. The discussion is extended to an examination of TGA-QD clusters in solutions with varying volumes of cysteamine and monodispersed monolayers of TGA-QDs.

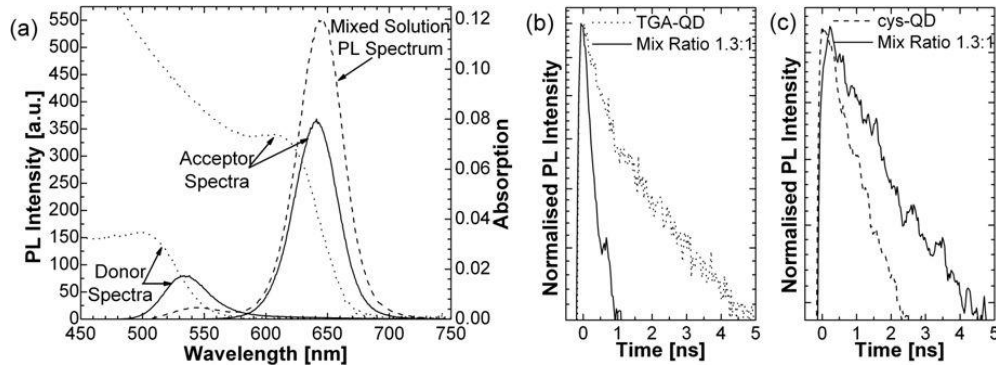


Fig. 1. (a) Photoluminescence (PL) (solid line, left-hand axis) and absorption (dotted line, right-hand axis) spectra of the pure donor TGA-QDs and the pure acceptor cys-QDs in aqueous solutions. PL (dashed line) spectrum of a mixed solution, ratio 1.3:1, of TGA-QDs and cys-QDs at the same concentrations as in the respective pure solutions. (b) Time resolved PL (TRPL) measurements of the donor QDs in a pure solution (dotted line) and in mixed solution (solid line), recorded using a filter centred at 500 nm. (c) TRPL measurements of the acceptor QDs in a pure solution (dashed line) and in mixed solution (solid line), recorded using a filter centred at 700 nm.

The photoluminescence spectra and time-resolved photoluminescence decays for pure and mixed donor and acceptor solution at a single concentration ratio are presented to highlight the signatures of FRET in both the spectral and temporal domains. Figure 1(a) shows the absorption and PL spectra of a pure TGA-QD donor solution with concentration $c_{Don} = 9.4 \times 10^{-7} \text{ M}$ and a pure cys-QD acceptor solution with concentration $c_{Acc} = 7.5 \times 10^{-7} \text{ M}$. A Förster radius (R_0) of 3.9 nm was calculated from the spectral overlap of the donor QD emission and acceptor QD absorption [6]. It should also be noted that there

is overlap between the blue side of the donor emission spectrum and the donor absorption spectrum. This overlap can lead to donor-donor intra-ensemble energy transfer [16]. A Förster radius of 3.0 nm was calculated in this case. Also shown is the spectrum for a mixed solution of the same concentrations of donor and acceptor QDs. A prerequisite for FRET is the close proximity of the donor and acceptor QDs, which is achieved in the mixed solution via the formation of nanoclusters through electrostatic interaction of oppositely charged QDs. The PL spectra show a clear increase of the acceptor emission and quenching of the donor emission. Figure 1(b) shows the TRPL decay curves of the donor QDs. The donor lifetime is reduced from 13.5 ns in the pure TGA-QD donor solution to 5.6 ns in the mixed solution with a donor: acceptor ratio of 1.3:1. The acceptor decay curves are shown in Fig. 1(c). The acceptor lifetime in the mixed solution is seen to increase to 16.0 ns compared to a lifetime of 13.8 ns in the pure cys-QD solution. Donor and acceptor QD TRPL decay curves were measured over the range of donor:acceptor ratios. For all mixed solutions the PL lifetime of the donor QDs is reduced relative to the pure donor solution of the same donor QD concentration and the lifetime of the acceptor QDs is increased. The donor PL decays at donor:acceptor concentration ratios of 1:1, 1.5:1, 4.5:1 and 7:1 are shown in the inset of Fig. 3(a). The donor PL quenching and acceptor PL enhancement, together with the TRPL lifetime data, which will be discussed in detail later, are all signatures of FRET from the donor QDs to the acceptor QDs in the nanoclusters formed in the mixed solution.

The dependence of the donor emission quenching and the acceptor emission enhancement on the donor: acceptor ratio are presented in Fig. 2. The donor emission quenching in the mixed solutions with reference to pure donor solutions of the same concentrations is quantified by $Q = I_{Dmix}/I_{Dref}$, where I_{Dref} and I_{Dmix} are the integrated donor TRPL intensities in the pure and the mixed solutions, respectively. Similarly, the enhancement of the acceptor emission is given by $E = I_{Amix}/I_{Aref}$, where I_{Aref} and I_{Amix} are the integrated acceptor TRPL intensities in the pure and the mixed solutions, respectively.

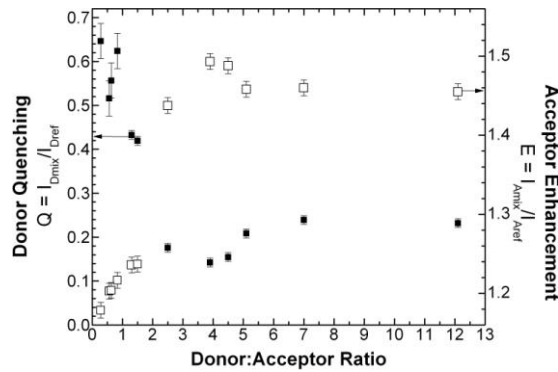


Fig. 2. Left-hand axis: PL quenching of the donor TGA-QD integrated time resolved photoluminescence (TRPL) as a function of the ratio of the number of donor QDs to acceptor QDs. Right-hand axis: PL enhancement of the acceptor cys-QD integrated TRPL as a function of the donor: acceptor ratio.

As can be seen in Fig. 2, in the mixed solution with a donor: acceptor ratio of 0.28:1, the lowest ratio investigated, the donor signal is quenched to ~60% of its original value. The donor quenching (solid symbols) remains at this level up to a donor: acceptor ratio of 0.86:1. As the donor: acceptor ratio is further increased to 1.3:1 the donor emission is quenched to ~43% of the reference value, close to what is expected for a Förster radius of 3.9 nm and a donor to acceptor centre to centre distance of 3.6 nm. The centre to centre distance is calculated taking account of the radii of each QD and the length of the interpenetrating ligand shells. As the donor: acceptor ratio is further increased the donor emission is further

quenched decreasing to a minimum of ~15% of the reference value for a ratio of 4 donors per acceptor. At higher donor: acceptor ratios, the donor emission recovers slightly and reaches a plateau at ~23%. The acceptor PL enhancement (clear symbols) is also shown in Fig. 2 and it can be noted that its dependence on the donor: acceptor ratio follows the opposite trend to that observed for the donor quenching. For low donor: acceptor ratios, in the range 0.28:1 to 1:1, there is only a low level of acceptor enhancement as the solution is dominated by free acceptors. As the donor: acceptor ratio increases, the acceptor PL signal is enhanced to a maximum of ~150% at a donor: acceptor ratio of ~4:1. Again at higher donor concentrations the enhancement levels off, suggesting that the maximum number of donors that can attach to a single acceptor has been achieved. From geometric considerations it is possible to estimate the number of donors that can form a closely packed shell around a single acceptor QD by calculating the number of times the cross-sectional area of a donor QD can fit on the surface area of the larger sphere with radius 3.6 nm, equal to the sum of the radius of the acceptor QD, the radius of the donor QD and the ligand length of 0.5 nm. The ligand length is included just once to account for interpenetration of the donor and acceptor QD ligand shells. Due to the amount of unoccupied space when packing spheres, the cross-sectional area of the donor QD is considered as a square with each side of length 2.9 nm, equal to the diameter of the donor QD and the length of the TGA ligand. Again the ligand length is only included once to allow for interpenetration of the donor ligand shells. These considerations suggest up to 19 donor QDs could surround a single acceptor. However, the zeta potential measurements support the formation of clusters with a maximum of 4 to 5 donors packing around a single acceptor, the ratio at which their opposite surface charges are compensated. Nanoclusters comprised of multiple donors attached to a single acceptor in solutions of oppositely charged QDs have been previously reported [12].

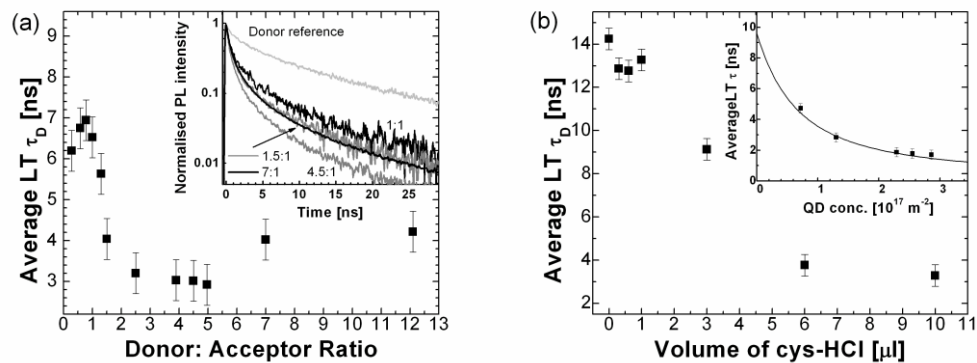


Fig. 3. (a) The average donor lifetime (LT) as a function of the number of the number of donor QDs per acceptor QD in mixed solutions. The average lifetime for a pure donor QD solution is 14ns. The measured PL decays at four donor:acceptor ratios are shown in the inset. (b) The average lifetime for TGA-QD solutions as a function of cys-HCl volume. Inset: Measured (squares) and calculated (line) lifetime as a function of TGA-QD concentration in the LbL-deposited monolayers.

The average donor lifetime as a function of the donor: acceptor ratio in the mixed solution is shown in Fig. 3(a). It can be noted that the donor lifetime and donor quenching show a similar dependence on the donor: acceptor ratio. For ratios up to 1:1, the average lifetime is approximately 6 ns. As the donor: acceptor ratio increases the average donor lifetime decreases to a minimum of 3.0 ns at a ratio of 5:1. Further increasing the donor concentration and the corresponding donor: acceptor ratio, results in a slight increase in the donor lifetime to 4.0 ns, which remains at this value at higher donor concentrations. The donor concentration independent lifetime in the ratio range up to 1:1 suggests that for these ratios every donor is attached to an acceptor. Due to the higher charge of the acceptors the formation of clusters

containing multiple acceptors is unlikely. Therefore, this donor concentration independent donor lifetime reflects predominantly the donor to acceptor FRET process in clusters formed from a single donor and single acceptor. As the donor concentration is further increased the additional donors can either remain free in solution, which would result in an increase of the measured donor lifetime, or the additional donors can attach to acceptors forming nanoclusters with multiple donors per acceptor. The donor to acceptor FRET rate is dependent only on the number of acceptors available to any given donor and is independent of the number of donors [3]. Therefore, when the donor lifetime is only determined by the donor to acceptor FRET process, attaching more than one donor to a single acceptor should not cause a further decrease of the donor lifetime. Consequently, the further reduction of the donor lifetime in the ratio range 1:1 to 5:1 is most likely due to donor-donor intra-ensemble energy transfer, as has already been observed in monodispersed QD monolayers [16]. Donor to donor FRET is facilitated by the inhomogeneous broadening of the donor QD ensemble, which results in an overlap of the emission spectrum of the smaller donor QDs on the blue side of the ensemble emission spectrum with the absorbing states of the larger donor QDs. The probability for this energy transfer mechanism increases as the donors come into closer proximity on attaching to a single acceptor. Donor to donor FRET has been further investigated for the donors used in this study through characterisation of both donor-only clusters and Layer-by-Layer assembled monolayers with varying TGA-QD concentration, which will be discussed further below.

As noted above, the minimum lifetime and maximum donor quenching both occur for a ratio of four to five donors per acceptor, suggesting a maximum of 4 or 5 donors attach to a single acceptor. It could therefore be expected that further increases in the donor concentration should increase the number of free donors in the mixed solution and result in an increase in the measured donor lifetime with a corresponding increase in the donor emission. However, as discussed above, while the average lifetime initially increases it quickly levels off at a value of approximately 4 ns, which is below the lifetime measured in the mixed solution with the lowest donor concentrations or in the pure donor reference solution. Similarly, at the higher donor concentrations the donor emission, calculated from the integrated TRPL recorded at 500 nm on the blue side of the donor emission spectrum, remains quenched in the mixed solutions, as shown in Fig. 2. This is attributed to the formation of donor QD clusters due to the presence of cysteamine in the mixed solution. The impact of cysteamine on the donor TGA-QDs can be observed via measurement of the TRPL lifetime of a pure TGA-QD solution as a function of the added volume of cysteamine, as shown in Fig. 3(b). In the absence of any cysteamine the donor reference lifetime in the pure TGA-QD solution is 14 ns. The TGA-QD lifetime decreases as increasing volumes of cysteamine are added to the pure TGA-QD solution. The addition of the positively charged cysteamine would facilitate the formation of TGA-QD clusters. The decreasing lifetime is consistent with increased donor to donor FRET as would be expected within clusters of TGA-QDs. The donor QD lifetime is reduced to 3.3 ns for 10 μ L of cysteamine added to a 3 mL solution of pure TGA-QDs with a QD concentration of 7.5×10^{-7} M. It can be noted that the lifetimes measured in the pure TGA-QD solution containing cysteamine are comparable to those observed at the higher donor QD concentrations in the mixed TGA-QD donor and cys-QD acceptor solutions. It should also be noted that the FRET efficiency should not be calculated directly from the ratio of the donor lifetimes in the pure and mixed solutions due to the influence of the cysteamine in the mixed solution.

Donor to donor FRET for the TGA-QDs can be further investigated by studying monolayers for a range of QD concentrations, as has been described in detail in reference [16]. The monolayers were prepared using the Layer-by-Layer assembly technique [6,16]. The inset of Fig. 3(b) shows TRPL (squares) lifetime data as a function of the TGA-QD concentration in the monolayer. The lifetime is seen to decrease with increasing

concentration. The solid line shows the results of a theoretical model for FRET for a random distribution of donors and acceptors in a monolayer. The larger lower energy QDs can act as acceptors for energy transfer from the smaller higher energy QDs within the inhomogeneously broadened TGA-QD ensemble. A full explanation of the theory has been given elsewhere [16]. The fitting parameters are the Förster radius $R_0 = 3.0 \pm 0.3 \text{ nm}$, the exclusion radius $R_{ex} = 2.8 \pm 0.3 \text{ nm}$, and the initial lifetime $\tau_0 = 9.6 \pm 0.5 \text{ ns}$. The value for R_0 is in good agreement with the Förster radius calculated from the overlap of the donor emission and donor absorption spectra, as discussed earlier. The exclusion radius is the minimum separation that can be achieved between two donors. The parameter, R_{ex} , is in good agreement with the distance of 2.9 nm calculated taking account of the radius of the donor QD and the interpenetration of the ligand shells. The initial lifetime refers to the donor lifetime in the absence of energy transfer. As can be seen the experimental data is well described by the theory and the fit parameters agree well with those calculated from the spectral data and the physical dimensions of the QDs, verifying that the concentration dependent decrease in lifetime can be attributed to FRET within the TGA-QD ensemble. The trend of the concentration dependence of the TGA-QD lifetime in both the pure TGA-QD solutions containing cysteamine and the mixed solutions of donor:acceptor ratios up to 5:1 is similar to the decreasing lifetime observed in the monolayers. This further suggests that the decrease in the TGA-QD lifetime in the mixed solutions is a consequence of energy transfer between the TGA-QD donors in the ratio range 1:1 to 5:1 where nanoclusters comprising multiple donors around a single acceptor are likely to be formed. Therefore, the decrease in TGA-QD lifetime in the mixed solutions over this range is not a signature of increased donor to acceptor FRET.

Care has to be taken in the analysis of FRET efficiencies from the lifetime data. It can be noted that at the lowest donor concentrations, where the clusters formed are predominantly comprised of a single donor attached to a single acceptor and the probability of all-donor cluster formation is low, there is good agreement between the FRET efficiency of ~60% calculated from the Förster radius $R_0 = 3.9 \text{ nm}$, taking a centre to centre donor-acceptor separation of 3.6 nm, with that calculated from the ratio of the donor lifetimes in the pure and mixed solutions, 14 ns and 6 ns respectively. The 14 ns represents the average reference lifetime and 6 ns is the average lifetime at low donor:acceptor concentration ratios in the mixed solution. However, as the donor concentration increases the lifetime in the pure solution is no longer a valid reference for the calculation of the FRET efficiency as it neglects the concentration dependent donor to donor energy transfer in either donor-acceptor clusters with multiple donors or in all-donor clusters. As discussed earlier this is also sensitive to the amount of excess cysteamine in the mixed solution.

4. Conclusion

In this study we have investigated QD nanoclusters in aqueous solution formed using oppositely charged donor and acceptor CdTe QDs. FRET with a donor quenching efficiency of approximately 50% has been observed in mixed solutions of QDs with oppositely charged TGA and cysteamine ligand shells. A maximum quenching of the donor PL to 15% of the emission of a pure donor solution and acceptor PL enhancement by a factor of 1.5 is observed for a ratio of four to five donors per acceptor. The donor emission quenching, acceptor emission enhancement and donor lifetime data all indicate that this is the maximum number of donor QDs per acceptor, consistent with the zeta potential measurements. The concentration dependence of the donor QD lifetime in the ratio range 1:1 to 5:1 is thought to be a signature of donor-donor energy transfer, as has been previously observed in solid planar systems [16], and should not be misinterpreted as a concentration dependence of the donor to acceptor energy transfer. The concentration dependent donor lifetime is therefore reflecting

the different types of clusters formed in solution, which apart from donor:acceptor clusters also contains pure donor-clusters, formed by the excess cysteamine in the solution, at high donor:acceptor ratios.

Acknowledgement

This work was financially supported by Science Foundation Ireland 05/PICA/1797.